Journal of Membrane Science & Research

journal homepage: www.msrjournal.com

Research Paper

Manufacture of Layered-type MF Ceramic Membrane for Advanced Wastewater Treatment and its Fouling Control using Modularized Mechanical Scraper

Chan-Young Yun [1], Dong-Jin Son [2], Dae-Gun Kim [3], Jihyang Kweon [4], Ki-Ho Hong [4,*]

[1] *Department of Environmental Engineering, Konkuk University, Seoul, Republic of Korea*
[2] *Division of Water Supply and Sewerage Research, National Institute of Environmental Research, Incheon, Republic of Korea*
[3] *Materials & Membranes Co., Ltd., Gangnung-si, Gangwon-do, Republic of Korea*
[4] *Department of Civil and Environmental Engineering, Konkuk University, Seoul, Republic of Korea*

Article info

Received 2021-07-13
Revised 2021-09-07
Accepted 2021-09-07
Available online 2021-09-07

Keywords

Ceramic membrane
Microfiltration (MF)
Fouling control
Mechanical scraping
Permeability

Highlights

- Novel layered-type MF ceramic membrane for advanced WWT.
- Performances of filtration and mechanical scraping were evaluated.
- Turbidity of all the permeates were below 0.01 NTU.
- Mechanical scraping showed superior performance in preventing fouling and in recovering flux.
- Continuous scraping is highly suited to the prevention of membrane fouling.

Graphical abstract

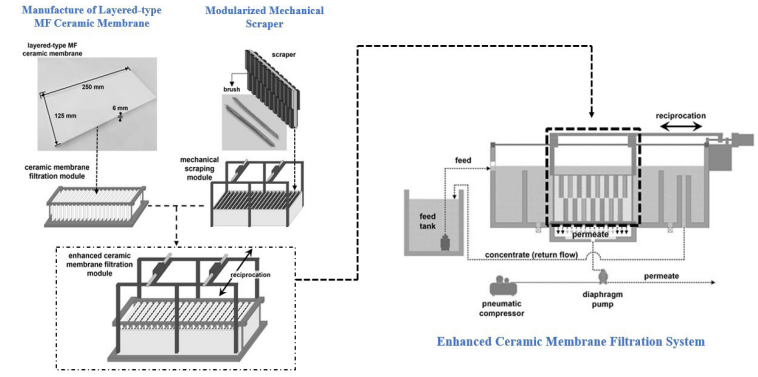

Abstract

In this study, a novel layered-type microfiltration (MF) ceramic membrane for advanced wastewater treatment was fabricated; composed of the support, buffer layer, and active layer. The buffer and active layers allow for the easy formation of the active layer on the support and selective permeation of the ceramic membrane, respectively. The average pore sizes of the support, buffer layer, and active layer were 2,677, 773.3, and 33.1 nm, respectively. The diameters of the active layer pores were <0.1 μm. The ceramic membrane performance and mechanical scraping effects on the membrane permeability improvement were evaluated. Mixed liquor suspended solids (MLSS) were used for the feed of an enhanced ceramic membrane filtration system, by combining the fabricated membranes and devised scrapers. The average flux recovery by scraping was 54% of the clean water flux; maintained by scraping despite the high turbidity feed. The permeation concluded within 0.2 h during scrape-off. This was not recovered despite scraping because the internal membrane pores became blocked due to the material turbidity and could not be separated at the surface of the ceramic membrane.

1. Introduction

In recent years, membranes have been used in numerous industrial fields; they can also be applied to the environmental industry. Specifically, membranes are utilized in advanced wastewater treatment and reuse. Currently, Polymeric membranes are mainly used, of either hollow-fiber or flat-sheet type. However, polymeric membranes for wastewater treatment are problematic due to issues such as their low durability and hydrophobicity [1]. These problems have not been solved despite the development of new materials (e.g., polyvinylidene fluoride (PVDF) and polytetrafluoroethylene (PTFE)), improving the membrane by surface-modification, or modifying processes such as pre-treatment of the feed stream, fluidized beds, and fluid instability [2,3].

Ceramic membranes are made of inorganic materials, such as alumina, zirconia, and titania [4,5], and is applicable for operation under high pressure conditions due to its excellent mechanical strength. Ceramic membranes are not damaged by chemical cleaning because they have high chemical durability [4-7]. Ceramic materials are also hydrophilic, and thus ceramic membranes have high fluxes at low operating pressures, as well as superior recoveries of feed water. Therefore, ceramic membranes have garnered

* Corresponding author: khhong@konkuk.ac.kr (K.-H. Hong)

DOI: 10.22079/JMSR.2021.533978.1476

attention as next-generation membranes in R&D (Research and Development) and commercial applications.

There are various causes of decreasing membrane permeability. The permeability gradually decreases during membrane operation. The formation of a gel or cake layer on the membrane surface promotes an increase in the membrane resistance [8-10]. Adsorption of foulant that is smaller than the membrane pores lead to the blockage of the pores [9,10]. Concentration polarization is caused by an increase in the solid concentration near the membrane surface, and this is one of the main causes for decreased membrane permeability [8,9,11].

Membranes with decreased permeability can be restored by backwash or chemical cleaning [9,12]. Chemical cleaning involves immersing the membrane in chemical cleansers, such as acidic or alkaline solutions. Chemical cleaning is commonly performed in cases where the performance of the membrane cannot be recovered by physical cleaning. Backwashing is a general method for membrane flux recovery [9,12,13]. This method uses a reverse flow for detachment of the foulant blocking the membrane pores. Backwashing is performed periodically, and the membrane process should be paused during backwash.

Other cleaning methods for membranes include the use of ultrasonic waves and granular materials, such as plastic particles or sponge balls. Ultrasonic waves cause the vibration of the membrane, leading to the detachment of foulant from the membrane surface [3,9,12,14]. This may be simultaneously applied to filtration, thus resolving problems due to the detachment of foulant and concentration polarization. However, the ultrasonic waves are not suitable for large or modularized membranes. Ultrasonic waves can also affect the microorganisms in the membrane bioreactor (MBR), such as breaking flocs.

The method of cleaning membranes using granular materials is generally called the 'mechanical cleaning process (MCP)' and is now commonly used. Plastic particles or sponge balls that do not damage the membrane surface are used as the granular materials [12,15,16]. Particular controls are not required when using this method. However, it is important to construct the shape of the reactor so that it provides a high collision frequency of the granules to the membranes. The MCP does have a problem with the control of the granule motions in the reactor. The granular materials can get stuck in the dead space due to hydraulic problems. The granules may not always be homogeneously distributed in the reactor. Moreover, biofilm formation on the granular materials, by attachment of microorganisms, can occur during the biological treatment process. The physical characteristics of the granules may change, and this can lead to the deterioration of the cleaning performance. The MCP cannot be used for ceramic membranes because its fouling control method is based on the membrane vibration due to collisions of the granules. A scraper is a device that directly cleans the membrane surface by preventing attachment of microorganisms or detaching foulant. Scraping is possible during filtration and is easy to automatize because of its simple principle. The operation may be also controlled by a mechanical device and is applicable to the cleaning process of ceramic membranes.

In this study, a ceramic membrane consisting of multiple layers was fabricated, and a system was devised by combining the membrane with a modularized scraper. Physical characteristics of the layered-type microfiltration (MF) membrane were assessed, and the performance of fouling control of the membrane by scraping was evaluated.

2. Materials and methods

2.1. Materials

Aluminum Oxide (α-Al_2O_3, Zhengzhou YUFA Abrasives Group Co., Ltd., China, average primary particle size = 50 nm) was the main materials used for preparing the support layer, buffer layer, and active layer of membranes. Methyl Cellulose as water soluble binder was purchased from Aldrich Chemical Co. (WI, USA). Deionized water was also used with Methyl Cellulose for manufacturing the support layer of membranes. Polyvinyl butyral (Sekisui, Japan) and butyl carbitol (Dow Chemical, USA) were used for preparing the buffer and active layers of membranes, and UAN (urethane acrylate non-ionomer, Aldrich Chemical Co., WI, USA) was also used as a dispersant for residence of the deposition and agglomeration of foulants onto the membrane surface. In addition, SiO_2 sol (Materials and Membranes Co. Ltd., 30nm) was applied for coating the active layer of membranes.

2.2. Preparation of layered-type MF ceramic membrane

The layered-type microfiltration ceramic membrane consists of a support, a buffer layer, and an active layer. In general, the support plays a role as the core of the ceramic membrane. It requires a large pore size and high porosity to maximize the permeability. However, an increase in pore size, leads to a reduction in the membrane's mechanical strength [17]. Therefore, both the mechanical strength and porosity should be considered during fabrication of the ceramic membrane. The slurry for support was synthesized by blending α-Al_2O_3 of 54 V/V%, H_2O of 27 V/V%, water soluble binder of 18 V/V%, and deforming agent with dispersant of 1 V/V% with a water bath at 40°C. A porous material was immersed in the synthesized slurry, and the material filled with the slurry was dried by an air blower at room temperature. The dried material was sintered at 1,300 °C for 2 h. The heating rate was 1°C/min. The sintered material was cooled at room temperature and was used as the support of the ceramic membrane. A flow chart for the fabrication of ceramic membrane is drawn in Figure 1.

Selective permeation of the ceramic membrane is determined by the active layer. The active layer has a lower permeability than that of the support, because the active layer has smaller pores. Thus, as the active layer is thinner, the ceramic membrane has better permeability. The procedure of coating the active layer is a key-step in the fabrication of ceramic membranes. It is technically difficult to coat the active layer on the support due to the differences in the pore sizes of the support and active layer. Therefore, a buffer layer must be coated on the support before the active layer is coated. However, the thickness of the buffer layer should be minimized because the buffer layer also influences the permeability of the membrane. The support was coated with slurry, for the buffer layer, by screen printing. Then it was sintered at 1,200℃ for 2 h with a heating rate of 1℃/min. The slurry for the buffer layer was synthesized by mixing α-Al_2O_3, polyvinyl butyral, butyl carbitol, and dispersant. The support coating with the buffer layer was coated with slurry for the active layer (mixture of α-Al_2O_3, SiO_2 sol, polyvinyl butyral, butyl carbitol, and dispersant) by screen printing. The layered-type ceramic membrane was completely fabricated by sintering the support coating with the active layer at 1,050℃ for 2 h with a heating rate of 1℃/min. The thickness of the support was 5.9 mm, and both the buffer and active layers were less than 0.1 μm, verified by an SEM image of the fabricated ceramic membrane.

2.3. Enhanced ceramic membrane filtration system

Schematic diagrams of the enhanced ceramic membrane filtration system are illustrated in Figure 2. The chamber of the system was made of Plexiglas, with 40 L of effective volume containing the ceramic membrane filtration module. The module was installed above a permeate collector that related to a diaphragm pump driven by a pneumatic compressor.

The enhanced ceramic membrane filtration module consisted of the ceramic membrane filtration and mechanical scraping modules. The module was equipped with 20 layered-type ceramic membranes with 10 mm intervals. The membranes were fixed by a metallic frame for preventing deviations due to external forces. The mechanical scraping module was equipped with 21 scrapers with 10 mm intervals. The brushes were made of densely packed polypropylene mohair (JAEIL Industry Co. Ltd) and attached to the scrapers. The surface of the membranes was scraped by the reciprocation action of the scrapers. The hairs on the brush were 10 mm long with a thickness below 50 μm. Although it was difficult to measure accurately the density of hairs attached on the brush, it was within geometric dimensioning and tolerancing because the hair was manufactured through a mechanical assembly process. The driving speed of the scrapers could be controlled by a variable speed motor. The driving speed was in the range 15–20 mm/s, and the driving range was 25 mm.

The feed consisted of mixed liquor suspended solids (MLSS) collected from the membrane bioreactor (MBR) in a separated sewered wastewater treatment plant which has a capacity below 500 ton/d in Gangwon, Korea. The concentration of the feed was controlled by settling or dilution. The feed was deposited by a submerged pump. The filtration was performed by depressurization, and the depressurizing parts consisted of a diaphragm pump and pneumatic compressor. The pressure of the pneumatic compressor was kept in the range of 0.6–0.7 bar during the operation of the system.

2.4. Analytical methods

Field emission scanning electron microscopy (FE-SEM, HITACHI, S-4700) was used to analyze the surface and cross-section of the fabricated layered-type MF ceramic membrane. The total suspended solids (TSS) of the MLSS were measured as per the procedures in the Standard Methods for the Examination of Water and Wastewater [18], and the turbidity was measured by a turbidimeter (HACH, 2100N). The pore size distributions of the layered-type MF ceramic membrane were measured by mercury porosimetry (MICROMERITICS, Autopore IV9110).

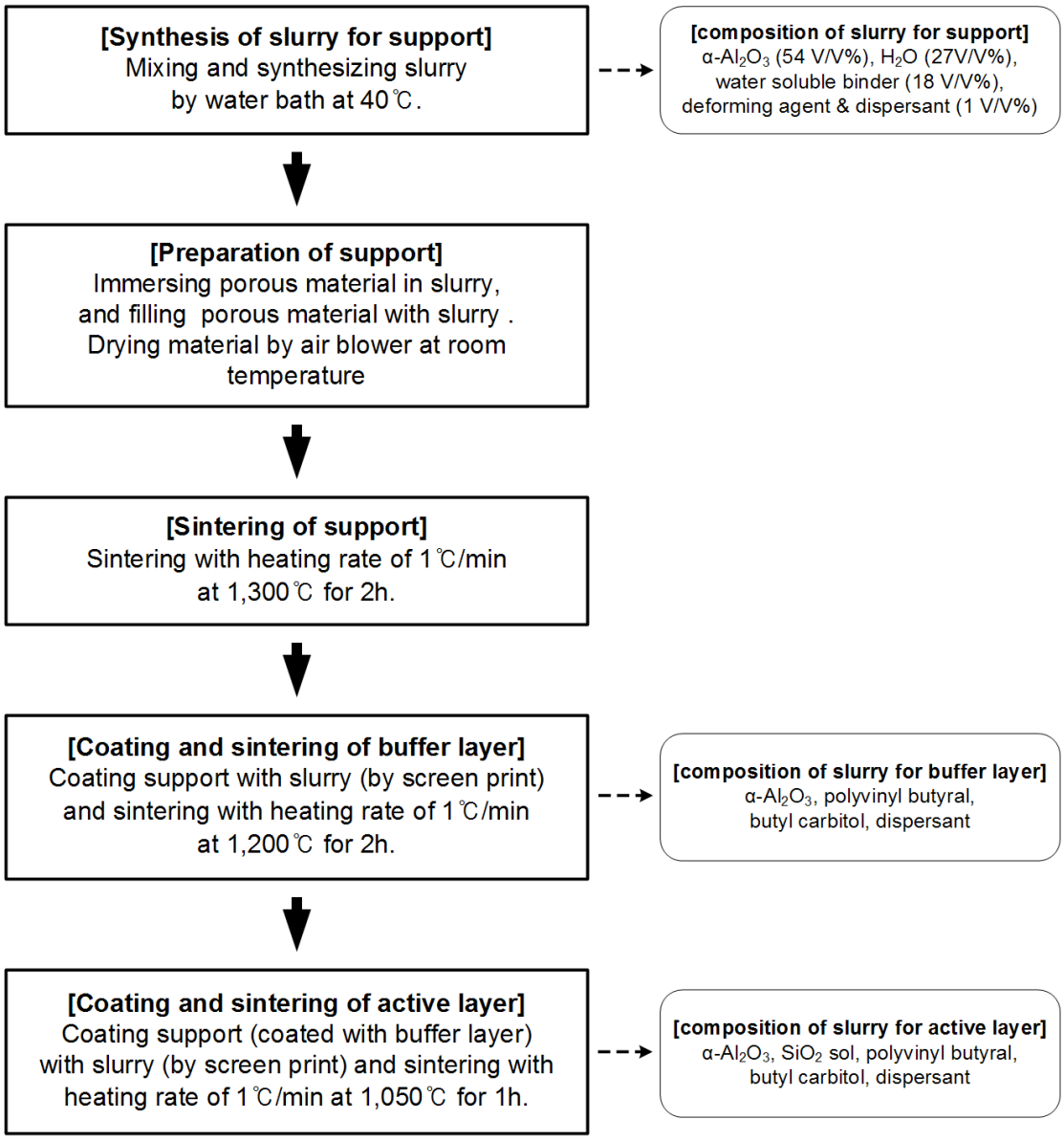

Fig. 1. Preparation steps and for layered-type MF ceramic membrane.

3. Results and discussion

3.1. Characteristics of layered-type MF ceramic membranes

In general, the structure of ceramic membranes is very important in guaranteeing mechanical strength as well as permeability. The support, acting as the core of the membrane, requires a large pore size and high porosity to maximize the permeability. However, an increase in the pore size causes a reduction in the membrane's mechanical strength. Therefore, the mechanical strength and porosity should be provided simultaneously when manufacturing the ceramic membrane. The active layer on the surface of the ceramic membrane plays an important role in selective permeation. The active layer has a lower permeability than that of the support because the active layer has smaller pores. Therefore, the thinner the active layer, the better the membrane permeability. The buffer layer must also be coated on the support before coating the active layer due to the differences in pore size between those of the support and active layer.

Figure 3 shows the cross-sectional scanning electron microscope (SEM) micrograph and surface morphology of our layered-type ceramic membrane. As presented in Figure 3a, both the buffer and active layers were stably coated onto the support and buffer layer, respectively. The support had a rougher structure than the other parts and was different to the typical porous structure. In general, a porous structure is a uni-body containing numerous pores. However, the support of our membrane had a structure characterized by lamination of the particles with heterogeneous sizes due to the support fabrication procedure. A porous material is melted, and the sintered slurry forms a support after sintering of the material filled with slurry. In other words, the particles shown in Figure 3a were sintered slurry that was filling the pores of the porous material, and the pores of the support are from the body of the porous material. This means that the pore characteristics, such as the pore size, porosity, and tortuosity, of the support can be controlled by the characteristics of the porous material which is used for the support fabrication. Figure 3b presents the surface structure of the active layer of the ceramic membrane, where many different pores with diameters of below 0.2 μm were found. The specific pore volume was measured by mercury porosimetry for the actual pore size distributions of each part in the fabricated layered-type ceramic membrane.

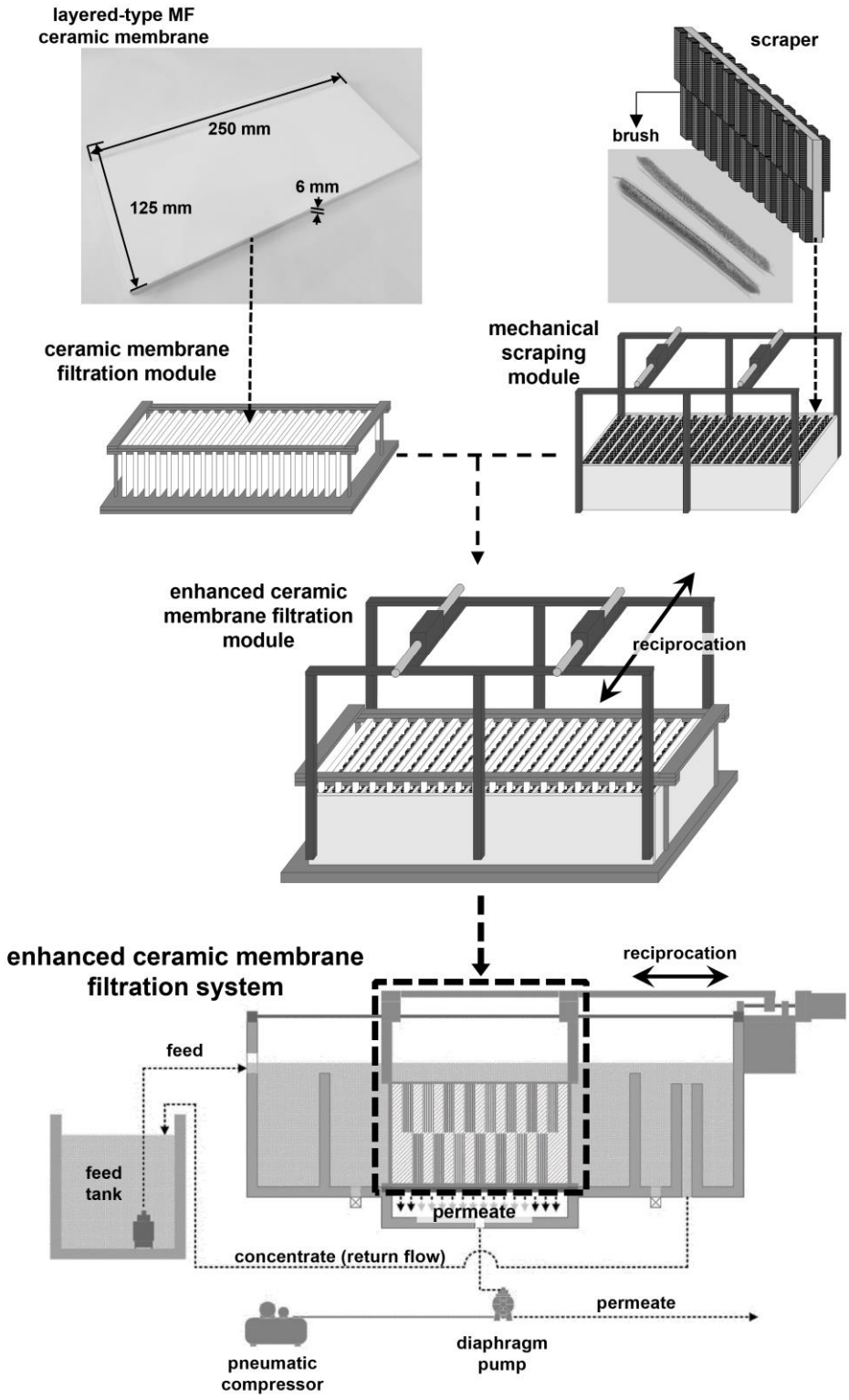

Fig. 2. Schematic diagrams of the enhanced ceramic membrane filtration system.

The pore size distributions of each part of the layered-type ceramic membrane are illustrated in Figure 4. The support and buffer layers contained macropores with diameters greater than 100 nm. The average pore sizes of the support and buffer layers were 2,677 and 773 nm, respectively. The pores of the active layer were mostly mesopores, other than some macropores with diameter greater than 50 nm, and the average size of the pores was 33 nm.

Figure 3a shows the cross-section of the membrane; the support had the most porous structure, with a porosity of 59.94%. However, the buffer layer was less porous than the active layer, and the porosities of the two layers were 41.19 and 48.73%, respectively. The reducing porosity of the buffer layer may have been caused by the coagulation of slurry particles in the pores of the buffer layer, near the boundary between it and the active layer. The coagulation could have occurred at the boundary between the support and buffer layers. However, it is believed that the porosity of the support was rarely reduced due to coagulation because the pores of the support were much bigger than those of the buffer layer.

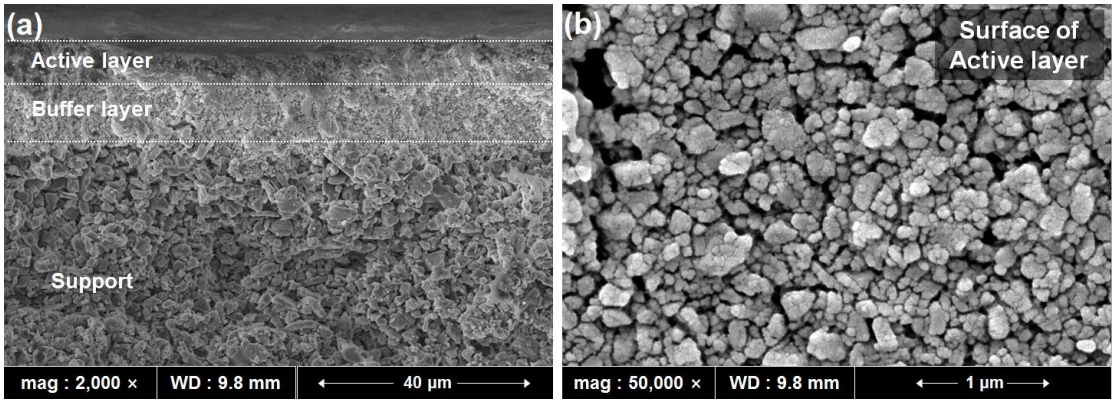

Fig. 3. SEM images of the (a) cross-section and (b) surface of the layered-type ceramic membrane.

3.2. Operations of the enhanced ceramic membrane filtration system

The changes in flux, depending on the concentration of MLSS, are depicted in Figure 5. The mechanical scraping module was driven during the initial 1 h, idled for 0.5 h, and driven for 0.5 h again. As the concentration of MLSS increased, the initial flux decreased compared with the clean water flux. During the initial 1 h of operation with scraping, the flux sharply declined within 0.1 h. The flux then stabilized after 0.5 h. The fluxes, prior to stopping the scrapers, were 103, 85, and 73 L/m^2/h for the three stages. The recovered fluxes were 97, 82, and 69 L/m^2/h, corresponding to 63, 54, and 45% of the clean water flux, and 72, 65, and 67% of the initial flux, respectively. Regardless of the scraping, the flux decrement was less than the results of other studies [19-21]. The corresponding turbidities of the feed were 16.2, 19.3, and 22.3 NTU. All the turbidities of the permeates were less than 0.01 NTU.

Under the condition of idling of the scraping module, the ratios of the fluxes to clean the water fluxes decreased to 0.52, 0.37, and 0.25, within 0.5 h when the concentrations of the MLSS were 1,030, 2,800, and 4,630 mg/L, respectively. Thus, simultaneously driving the mechanical scraping module with filtration had the enough effect of preventing the fouling of the ceramic membrane and maintaining the flux. In addition, the effects were more effective for higher MLSS concentrations. Moreover, intermittent scraping at intervals as well as simultaneous scraping during the whole operating time was superior for recovering the flux. As interval of the intermittent scraping is shorter, the flux could be maintained higher [22].

Figure 6 shows the limitation of the mechanical scraping for cleaning of the membrane surface. The MLSS concentrations of the cases were 4,630 and 5,460 mg/L, respectively. In general, membrane fouling could be affected by concentration of suspended solids significantly affects membrane flux [23-25], membrane materials, MLSS features, and operating conditions [26-29]. In this study, the flux decrements of both cases were restrained significantly by the scraping. When scraping idling was performed, the fluxes of both cases decreased rapidly. Permeation could not be performed for 5,460 mg/L of MLSS, and the flux was not recovered despite the scraping. The MLSS and turbidity of the supernatant were 41.1 mg/L and 22.3 NTU for 4,630 mg/L of MLSS, and 46.8 mg/L and 80.7 NTU for 5,460 mg/L of MLSS, respectively. Therefore, the particles with smaller diameters, compared with the pores of the active layer for 5,460 mg/L of MLSS, were more contained than those of the 4,630 mg/L case, and the particles entered the pores and blocked the channels, as same as the result of Zhang et al. [20]. The effects of the mechanical scraping module cannot be expected to recover the flux when the feed has a high quantity of MLSS and turbidity, which occurred for the particles with smaller diameters compared with the pores of the active layer. In this case, backwashing or chemical treatment would be required to recover the flux of membranes. From Chollom et al. [30], chemical treatment with the surface scraping recovered the flux to 93% while the scraping-only recovered 43%.

Figure 7 shows the SEM images of the cross-section and surface of the layered-type ceramic membrane that was scraped during operation. As shown in Figure 7a, the active layer was fouled, whereas the buffer layer and support were almost as clean as the unused membrane. However, Figure 7b shows the surface at a magnification of 50,000, and the pores were not completely blocked. This means that the mechanical scraping module prevented fouling of the pores by removing the foulant from the surface of the membrane. The cake layer on the membrane surface was not clearly removed despite utilizing the mechanical scraping module. The formation of the cake layer led to a decline in the flux by decreasing the pore size and increasing the membrane resistance. On the other hand, a decrease in the pore size enhances selective permeation. Therefore, mechanical scraping prevented the fouling of the membrane and also improved the solid-liquid separation ability of the membrane.

Figure 8 shows SEM images of the cross-section and surface of the layered-type ceramic membrane for a feed with a turbidity of 80.7 NTU. As previously shown in Figure 6, the permeation stopped within 0.2 h after scrape-off, and the flux had not recovered despite resuming the scraping. This may be explained by the fouling of the interior of the active layer, as shown in Figure 8a. The pores of the surface in Figure 8b were hardly observed, contrary to Figure 7b. This is due to the attachment of turbid materials and blockages of the membrane pores. Mechanical scraping can prevent the attachment of turbid material to the pores. However, the pores were already blocked, and the turbid material attachment could not be recovered despite the use of the mechanical scraper.

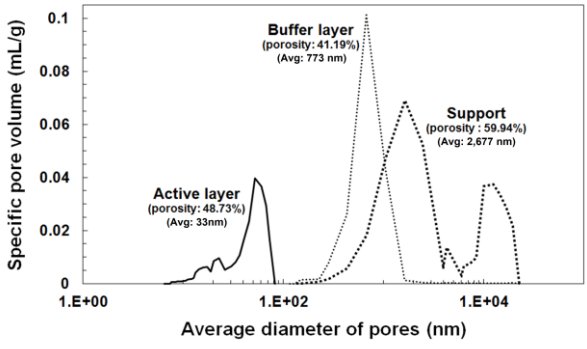

Fig. 4. Pore size distributions of the layered-type ceramic membrane.

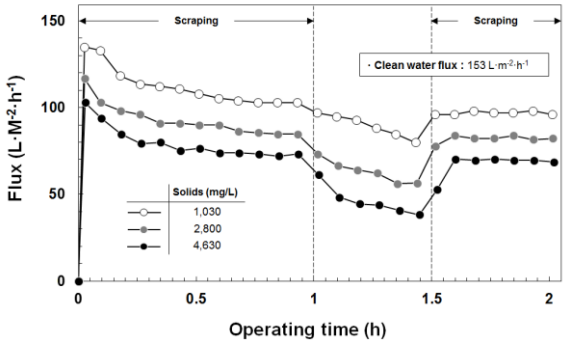

Fig. 5. Flux as a function of MLSS concentration and effect of scraping.

4. Conclusions

In this study, a layered-type MF ceramic membrane consisting of a support, buffer layer, and active layer was manufactured in a satisfactory manner. A mechanical scraper was also designed to enhance the permeability of the membrane. Effects of the mechanical scraping were evaluated through an enhanced ceramic membrane filtration system that combined the membrane and scraper.

The active layer was stably coated on the support due to the buffer layer. The fabricated membrane satisfied the specifications of microfiltration. The turbidity of all the permeates were below 0.01 NTU during the operations. Thus, the fabricated layered-type ceramic membrane was functionally perfect for microfiltration in advanced wastewater treatment.

The mechanical scraping showed superior performance in preventing fouling and in recovering flux. The flux was constantly maintained by simultaneous scraping with filtration. The recovery rate of the flux averaged 68% of the saturated flux after the idling scrapers for 0.5 h, before resuming. It should be noted that intermittent scraping was also acceptable for maintaining the membrane, as well as for simultaneous scraping with filtration. Easy maintenance of the membrane would be promoted by intermittent operation through fouling prevention and recovery of flux, under the condition of a feed with a low solid concentration that cannot be separated at the ceramic membrane surface. Thus, mechanical scraper would be another option for the continuous of membrane facilities in the wastewater treatment plants suffering the fouling of the membrane.

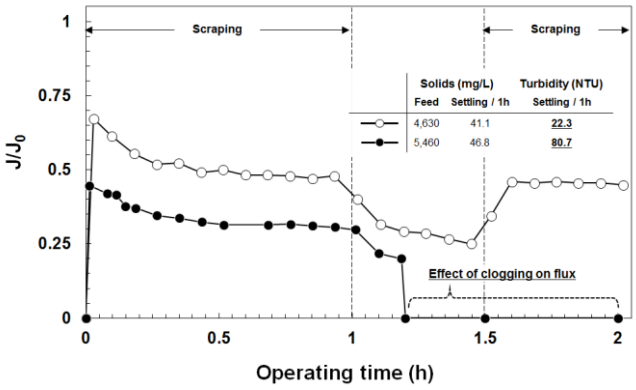

Fig. 6. Limitation of scraping surface for fouling control.

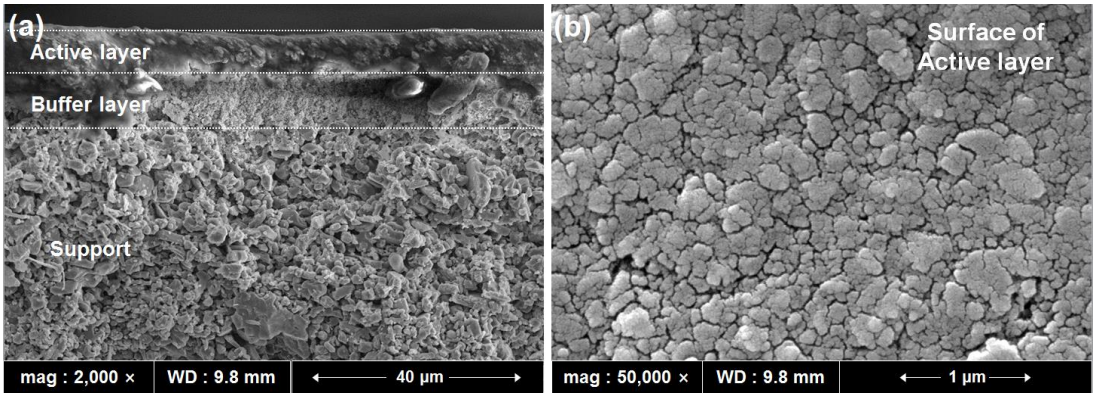

Fig. 7. SEM images of the (a) cross-section and (b) surface of the layered-type ceramic membrane with mechanical scraping.

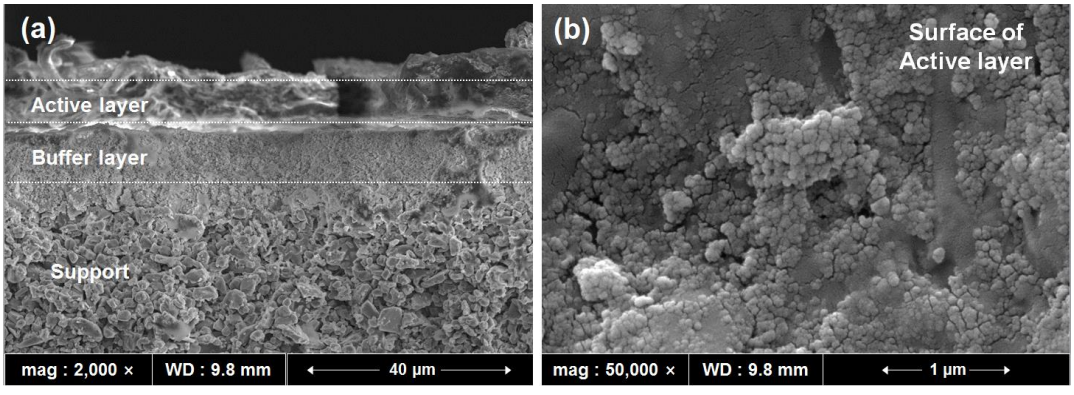

Fig. 8. SEM images of the (a) cross-section and (b) surface of the fouled layered-type ceramic membrane without mechanical scraping.

List of abbreviations

MF	MicroFiltration	MCP	Mechanical Cleaning Process
MLSS	Mixed Liquor Suspended Solids	SEM	Scanning Electron Microscope
PVDF	PolyVinyliDene Fluoride	MBR	Membrane BioReactor
PTFE	PolyTetraFluoroEthylene	TSS	Total Suspended Solids
R&D	Research and Development	NTU	Nephelometric Turbidity Units

References

[1] S.J. Lee, M. Dilaver, P.K. Park, J.H. Kim, Comparative analysis of fouling characteristics of ceramic and polymeric microfiltration membranes using filtration models, J. Membr. Sci. 432 (2013) 97-105. https://doi.org/10.1016/j.memsci.2013.01.013

[2] L. Xia, A.W.K. Law, A.G. Fane, Hydrodynamic effects of air sparging on hollow fiber membranes in a bubble column reactor, Water Res. 47 (2013) 3762-3772. https://doi.org/10.1016/j.watres.2013.04.042

[3] C.C. Kan, D.A.D. Genuino, K.K.P. Rivera, M.D.G. De Luna, Ultrasonic cleaning of polytetrafluoroethylene membrane fouled by natural organic matter, J. Membr. Sci. 497 (2016) 450-457. https://doi.org/10.1016/j.memsci.2015.08.031

[4] B. Hofs, J. Ogier, D. Vries, E.F. Beerendonk, E.R. Cornelissen, Comparison of ceramic and polymeric membrane permeability and fouling using surface water, Sep. Purif. Technol. 79 (2011) 365-374. https://doi.org/10.1016/j.seppur.2011.03.025

[5] ER. Fang, G. Qin, W. Wei, X. Zhao, L. Jiang, Elaboration of new ceramic membrane from spherical fly ash for microfiltration of rigid particle suspension and oil-in-water emulsion, Desalination. 311 (2013) 113-126. https://doi.org/10.1016/j.desal.2012.11.008

[6] X. Zhang, L. Fan, F.A. Roddick, Feedwater coagulation to mitigate the fouling of a ceramic MF membrane caused by soluble algal organic matter, Sep. Purif. Technol. 133 (2014) 221-226. https://doi.org/10.1016/j.seppur.2014.06.053

[7] B.G. Kunde, GD. Yadav, Sol–gel synthesis and characterization of defect-free alumina films and its application in the preparation of supported ultrafiltration membranes, J. Sol-Gel Sci. Technol. 77 (2016) 266-277. https://doi.org/10.1007/s10971-015-3852-8

[8] T.V. Nguyen, M.T.M. Pendergast, M.T. Phong, X. Jin, F. Peng, M.L. Lind, E.M.V. Hoek, Relating fouling behavior and cake layer formation of alginic acid to the physiochemical properties of thin film composite and nanocomposite seawater RO membranes, Desalination. 338 (2014) 1-9. https://doi.org/10.1016/j.desal.2014.01.013

[9] Z. Wang, J. Ma, C.Y. Tang, K. Kimura, Q. Wang, X. Han, Membrane cleaning in membrane bioreactors: A review, J. Membr. Sci. 468 (2014) 276-307. https://doi.org/10.1016/j.memsci.2014.05.060

[10] E. Poorasgari, T.V. Bugge, M.L. Christensen, M.K. Jørgensen. Compressibility of fouling layers in membrane bioreactors, J. Membr. Sci. 475 (2015) 65-70. https://doi.org/10.1016/j.memsci.2014.09.056

[11] A.A. Tashvigh, A. Fouladitajar, F.Z. Ashtiani, Modeling concentration polarization in crossflow microfiltration of oil-in-water emulsion using shear-induced diffusion; CFD and experimental studies, Desalination. 357 (2015) 225-232. https://doi.org/10.1016/j.desal.2014.12.001

[12] X. Shi, G. Tal, N.P. Hankins, V. Gitis, Fouling and cleaning of ultrafiltration membranes: A review, J. Water Process Eng. 1 (2014) 121-138. https://doi.org/10.1016/j.jwpe.2014.04.003

[13] Z. Cui, J. Wang, H. Zhang, H Jia, Influence of released air on effective backwashing length in dead-end hollow fiber membrane system, J. Membr. Sci. 530 (2017) 132-145. https://doi.org/10.1016/j.memsci.2017.02.014

[14] S.R. Gonzalez-Avila, F. Prabowo, A. Kumar, C.D. Ohl, Improved ultrasonic cleaning of membranes with tandem frequency excitation, J. Membr. Sci. 415-416 (2012) 776-783. https://doi.org/10.1016/j.memsci.2012.05.069

[15] S. Rosenberger, F.P. Helmus, S. Krause, A. Bareth, U. Meyer-Blumenroth, Principles of an enhanced MBR-process with mechanical cleaning, Water Sci. Technol. 64 (2011) 1951-1958. https://doi.org/10.2166/wst.2011.765

[16] M. Aslam, A. Charfi, G. Lesage, M. Heran, J. Kim, Membrane bioreactors for wastewater treatment: A review of mechanical cleaning by scouring agent to control membrane fouling, Chem. Eng. J. 307 (2017) 897-913. http://dx.doi.org/10.1016/j.cej.2016.08.144

[17] J.H. Ha, E. Oh, B. Bae, I.H. Song, The effect of kaolin addition on the characteristics of a sintered diatomite composite support layer for potential microfiltration applications, Ceram. Int. 39 (2013) 8955-8962. https://doi.org/10.1016/j.ceramint.2013.04.092

[18] APHA, Standard methods for the examination of water and wastewater, 22nd Ed., American Public Health Association, Washington D.C., 2012.

[19] J. Fang, G. Qin, W. Wei, X. Zhang, L. Jiang, Elaboration of new ceramic membrane from spherical fly ash for microfiltration of rigid particle suspension and oil-in-water emulsion, Desalination. 311 (2013) 113-126. https://doi.org/10.1016/j.desal.2012.11.008

[20] Q. Zhang, R. Xu, P. Xu, R. Chen, Performance study of ZrO_2 ceramic micro-filtration membranes used in pretreatment of DMF wastewater, Desalination. 346 (2014) 1-8. https://doi.org/10.1016/j.desal.2014.05.006

[21] C. He, R.D. Vidic, Application of microfiltration for the treatment of Marcellus Shale flowback water: Influence of floc breakage on membrane fouling, J. Membr. Sci. 510 (2016) 348-354. https://doi.org/10.1016/j.memsci.2016.03.023

[22] M.N. Chollom, S. Rathilal, K. Pikwa, L. Pillay, Fouling control in a woven fibre microfiltration membrane for water treatment, Environ. Eng. Res. 24 (2019) 418-426. http://dx.doi.org/10.1016/j.sajce.2016.12.003

[23] M. Saleem, L. Alibardi, R. Cossu, M.C. Lavagnolo, A. Spagni. Analysis of fouling development under dynamic membrane filtration operation, Chem. Eng. J. 312 (2017) 136-143. https://doi.org/10.1016/j.cej.2016.11.123

[24] M. Lousada-Ferreira, J.B. van Lier, H.J.M.J. van der Graaf, Impact of suspended solids concentration of sludge filterability in full-scale membrane bioreactors. J. Membr. Sci. 476 (2015) 68-75. https://doi.org/10.1016/j.memsci.2014.11.012

[25] C. Fu, X. Yue, X. Shi, K.K. Ng, H.Y. Ng, Membrane fouling between a membrane bioreactor and a moving bed membrane bioreactor: Effects of solids retention time, Chem. Eng. J. 309 (2017) 397-408. https://doi.org/10.1016/j.cej.2016.10.076

[26] R. Campo, M. Capodici, G. Di Bella, M. Torregrossa, The role of EPS in the foaming and fouling for a MBR operated in intermittent aeration conditions, Biochem. Eng. J. 118 (2017) 41-52. https://doi.org/10.1016/j.bej.2016.11.012

[27] S. Ishizaki, T. Fukushima, S. Ishii, S. Okabe, Membrane fouling potentials and cellular properties of bacteria isolated from fouled membranes in a MBR treating municipal wastewater, Water. Res. 100 (2016) 448-457. https://doi.org/10.1016/j.watres.2016.05.027

[28] H. Lin, M. Zhang, F. Wang, F. Meng, B.Q. Liao, H. Hong, J. Chen, W. Gao, A critical review of extracellular polymeric substances (EPSs) in membrane bioreactors: Characteristics, roles in membrane fouling and control strategies, J. Membrane. Sci. 460 (2014) 110-125. https://doi.org/10.1016/j.memsci.2014.02.034

[29] A. Drews, Membrane fouling in membrane bioreactors - Characterisation, contradictions, cause and cures, J. Membr. Sci. 363 (2010) 1-28. https://doi.org/10.1016/j.memsci.2010.06.046

[30] M.N. Chollom, K. Pikwa, S. Rathilal, V.L. Pillay. Fouling mitigation on a woven fibre microfiltration membrane for the treatment of raw water, S. Afr. J. Chem. Eng. 23 (2017) 1-9. https://doi.org/10.1016/j.sajce.2016.12.003